INFLATION AT THE EDGES

M. Kamionkowski[1]

RESUMEN

Resultados recientes de experimentos del fondo de microondas cósmico (FMC) prueban varias de las predicciones de la inflación y descartan muchos de los escenarios de formación cósmica alternativos. Dado el éxito de la teoría, el siguiente paso obvio es probar la inflación al filo de nuestras capacidades observacionales actuales y por venir. De acuerdo al paradigma inflacionario, las galaxies y su distribución a gran escala son remanentes de la inflación por lo que pueden ser estudiadas para explorarla más a fondo, de la misma manera que un físico de partículas experimental estudia los remanentes de colisiones de alta energía. A continuación haré un análisis de cómo estudios de subestructura galáctica, galaxias, cúmulos, estructura a gran escala y el FMC pueden ser usados para aprender más sobre la inflación.

ABSTRACT

Recent results from cosmic microwave background (CMB) experiments verify several of the predictions of inflation, while ruling out a number of alternative structure-formation scenarios. Given the successes of the theory, the obvious next step is to press ahead and test inflation to the edge of all our current and forthcoming observational abilities. According to the inflationary paradigm, galaxies and their large-scale distribution in the Universe are remnants of inflation and can thus be studied to learn more about inflation in the same way that experimental particle physicists study the remnants of high-energy collisions. Here I discuss how studies of galactic substructure, galaxies, clusters, large-scale structure, and the CMB, may be used to learn more about inflation.

Key Words: **COSMOLOGY**

1. INTRODUCTION

Inflationary cosmology (Guth 1981; Linde 1982a; Albrecht & Steinhardt 1982) has in recent years had a number of dramatic successes. The inflationary predictions of a flat Universe and nearly scale-invariant primordial density perturbations with Gaussian initial conditions (Guth & Pi 1982; Hawking 1982; Linde 1982b; Starobinsky 1982; Bardeen et al. 1983) have been found to be consistent with a series of increasingly precise cosmic microwave background (CMB) experiments (Miller et al. 1999; de Bernardis et al. 2000; Hanany et al. 2000; Halverson et al. 2002; Mason et al. 2002). Theorists discuss open-Universe and alternative structure-formation models, such as topological defects, with *far* less frequency than they did just three years ago.

Historically, when experimental breakthroughs confirm a particular theoretical paradigm and eliminate others, progress can be made at the edges—i.e., precision tests of the new standard model. In the case of inflation, a number of important questions should be addressed. For example, what is the physics responsible for inflation? What is the energy scale of inflation? In particular, we really do not understand why the simple slow-roll model of inflation—really no more than a toy model—works so well. Might deviations from the simplest model expected in realistic theories lead to small deviations from the canonical predictions of inflation? For example, is the density of the Universe precisely equal to the critical density? Are there deviations from scale invariance on small distance scales that arise as a consequence of the end of inflation? Might there be some small admixture of entropy perturbations in addition to the predominant adiabatic perturbations? Are there small deviations from Gaussian initial conditions?

A variety of forthcoming CMB experiments will test the flatness of the Universe with additional precision and determine the primordial spectrum of perturbations with increasing accuracy. CMB experiments and galaxy surveys and weak-lensing maps that determine the mass distribution in the Universe today will test Gaussian initial conditions. Our understanding of galactic substructure may shed light on the end of inflation. Experimentalists are beginning to contemplate programs to detect the unique polarization signature due to inflationary gravitational waves.

[1]California Institute of Technology, Pasadena, CA, USA

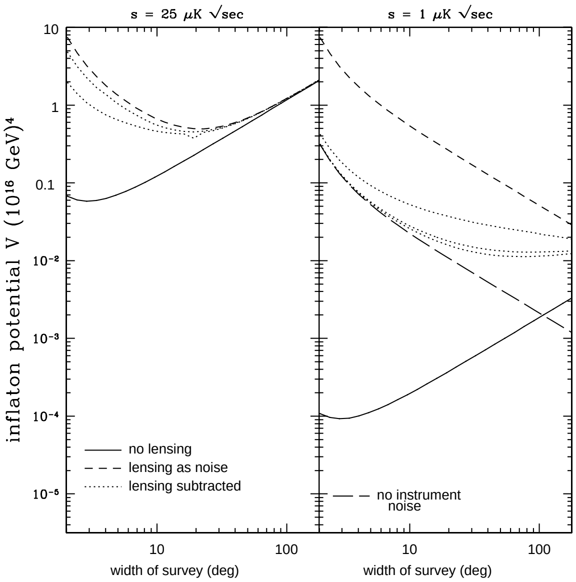

Fig. 1. Minimum inflaton potential observable at 1σ as a function of survey width for a one-year experiment. The left panel shows an experiment with NET $s = 25\,\mu\mathrm{K}\,\sqrt{\mathrm{sec}}$. The solid curve shows results assuming no CS while the dashed curve shows results including the effects of an unsubtracted CS; we take $\theta_{\mathrm{FWHM}} = 5'$ in these two cases. The dotted curves assume the CS is subtracted with $\theta_{\mathrm{FWHM}} = 10'$ (upper curve) and $5'$ (lower curve). Since the dotted curves are close to the dashed curve, it shows that these higher-order correlations will not be significantly useful in reconstructing the primordial curl for an experiment similar to Planck's sensitivity and resolution. The right panel shows results for hypothetical improved experiments. The dotted curves shows results with CS subtracted and assuming $s = 1\,\mu\mathrm{K}\,\sqrt{\mathrm{sec}}$, $\theta_{\mathrm{FWHM}} = 5'$, $2'$, and $1'$ (from top to bottom). The solid curve assumes $\theta_{\mathrm{FWHM}} = 1'$ and $s = 1\,\mu\mathrm{K}\,\sqrt{\mathrm{sec}}$, and no CS, while the dashed curve treats CS as an additional noise. The long-dash curve assumes CS subtraction with no instrumental noise ($s = 0$). From Kesden et al. (2002).

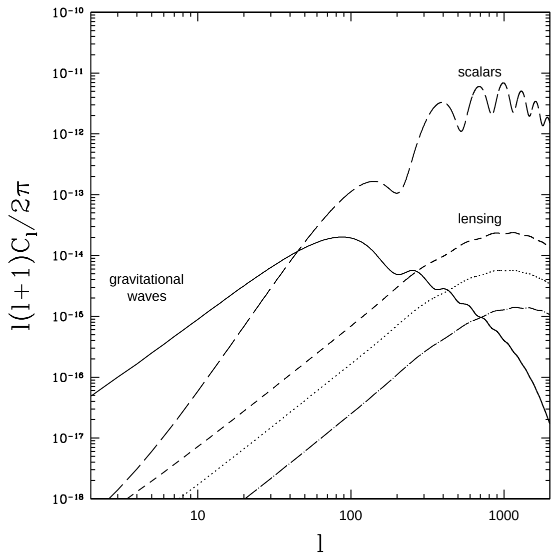

Fig. 2. CMB polarization power spectra. The long-dashed curve shows the dominant polarization signal in the gradient component due to scalar (density) perturbations. The solid line shows the maximum allowed curl polarization signal from the gravitational-wave background, which will be smaller if the inflationary energy scale is smaller than the maximum value allowed by COBE of 3.5×10^{16} GeV. The dashed curve shows the power spectrum of the curl component of the polarization due to CS. The dotted curve is the CS contribution to the curl component that comes from structures out to a redshift of 1; this is the level at which low-redshift lensing surveys can be used to separate the CS-induced polarization from the IGW signal. The dot-dashed line is the residual when lensing is separated with a no-noise experiment and 80% sky coverage. From Kesden et al. (2002).

Here, I briefly review several new probes of possible relics of inflation; namely inflationary gravitational waves, non-Gaussianity, and galactic substructure.

2. GRAVITATIONAL WAVES AND CMB POLARIZATION

One the most intriguing avenues toward further tests of inflation is the gravitational-wave background. In addition to predicting a flat Universe with adiabatic perturbations, inflation also predicts the existence of a stochastic gravitational-wave background with a nearly-scale-invariant spectrum (Abbott & Wise 1984). The amplitude of this inflationary gravitational-wave background (IGW) is fixed entirely by the vacuum-energy density during inflation, which is proportional to the fourth power of the energy scale E_{infl} of the new physics responsible for inflation.

Gravitational waves, like primordial density perturbations, produce linear polarization in the CMB. However, the polarization patterns from the two differ. This can be quantified with a harmonic decomposition of the polarization field. The linear-polarization state of the CMB in a direction $\hat{\mathbf{n}}$ can be described by a symmetric trace-free 2×2 tensor,

$$\mathcal{P}_{ab}(\hat{\mathbf{n}}) = \frac{1}{2} \left(\begin{array}{cc} Q(\hat{\mathbf{n}}) & -U(\hat{\mathbf{n}}) \sin\theta \\ -U(\hat{\mathbf{n}}) \sin\theta & -Q(\hat{\mathbf{n}}) \sin^2\theta \end{array} \right), \quad (1)$$

where the subscripts ab are tensor indices, and $Q(\hat{\mathbf{n}})$ and $U(\hat{\mathbf{n}})$ are the Stokes parameters. Just as the temperature map can be expanded in terms of spherical harmonics, the polarization tensor can be expanded (Kamionkowski et al. 1997a; Kamionkowski et al. 1997b; Seljak & Zaldarriaga 1997; Zaldarriaga & Seljak 1997),

$$\frac{\mathcal{P}_{ab}(\hat{\mathbf{n}})}{T_0} = \sum_{lm} \left[a^{\rm G}_{(lm)} Y^{\rm G}_{(lm)ab}(\hat{\mathbf{n}}) + a^{\rm C}_{(lm)} Y^{\rm C}_{(lm)ab}(\hat{\mathbf{n}}) \right], \tag{2}$$

in terms of tensor spherical harmonics, $Y^{\rm G}_{(lm)ab}$ and $Y^{\rm C}_{(lm)ab}$. It is well known that a vector field can be decomposed into a curl and a curl-free (gradient) part. Similarly, a 2×2 symmetric traceless tensor field can be decomposed into a tensor analogue of a curl and a gradient part; the $Y^{\rm G}_{(lm)ab}$ and $Y^{\rm C}_{(lm)ab}$ form a complete orthonormal basis for the "gradient" (i.e., curl-free) and "curl" components of the tensor field, respectively. The mode amplitudes in Eq. (2) are given by

$$\begin{aligned} a^{\rm G}_{(lm)} &= \frac{1}{T_0} \int d\hat{\mathbf{n}}\, \mathcal{P}_{ab}(\hat{\mathbf{n}})\, Y^{{\rm G}\, ab\, *}_{(lm)}(\hat{\mathbf{n}}), \\ a^{\rm C}_{(lm)} &= \frac{1}{T_0} \int d\hat{\mathbf{n}}\, \mathcal{P}_{ab}(\hat{\mathbf{n}})\, Y^{{\rm C}\, ab\, *}_{(lm)}(\hat{\mathbf{n}}), \end{aligned} \tag{3}$$

which can be derived from the orthonormality properties of these tensor harmonics (Kamionkowski et al. 1997b). Thus, given a polarization map $\mathcal{P}_{ab}(\hat{\mathbf{n}})$, the G and C components can be isolated by first carrying out the transformations in Eq. (3) to the $a^{\rm G}_{(lm)}$ and $a^{\rm C}_{(lm)}$, and then summing over the first term on the right-hand side of Eq. (2) to get the G component and over the second term to get the C component. The two-point statistics of the combined temperature/polarization (T/P) map are specified completely by the six power spectra $C_\ell^{\rm XX'}$ for ${\rm X}, {\rm X'} = \{{\rm T}, {\rm G}, {\rm C}\}$, but parity invariance demands that $C_\ell^{\rm TC} = C_\ell^{\rm GC} = 0$. Therefore, the statistics of the CMB temperature-polarization map are completely specified by the four sets of moments: $C_\ell^{\rm TT}$, $C_\ell^{\rm TG}$, $C_\ell^{\rm GG}$, and $C_\ell^{\rm CC}$.

Both density perturbations and gravitational waves will produce a gradient component in the polarization. However, to linear order in small perturbations, only gravitational waves will produce a curl component (Kamionkowski et al. 1997a; Seljak & Zaldarriaga 1997). The curl component thus provides a model-independent probe of the gravitational-wave background.

In Kamionkowski & Kosowsky (1998) and Jaffe et al. (2000), we studied the smallest IGW amplitude that can be detected by CMB experiments parameterized by a fraction of sky covered, the instrumental sensitivity (parameterized by a noise-equivalent temperature s), and an angular resolution. We found that the sensitivity to IGWs was maximized with a survey that covers roughly a $5^\circ \times 5^\circ$ patch of the sky (as indicated by the solid curve in Fig. 1) and with an angular resolution better than roughly 1°. The smallest detectable energy scale of inflation is then $E_{\rm infl} = 5 \times 10^{15} (s/25\,\mu{\rm K}\,\sqrt{\rm sec})^{1/2}$ GeV. For reference, the instrumental sensitivity for MAP is $O(100\mu{\rm K}\,\sqrt{\rm sec})$ and for the Planck satellite $O(20\,\mu{\rm K}\,\sqrt{\rm sec})$.

However, since then, it has been pointed out that cosmic shear (CS), gravitational lensing of the CMB due to large-scale structure along the line of sight, can convert some of the curl-free polarization pattern at the surface of last scatter into a curl component, even in the absence of gravitational waves (Zaldarriaga & Seljak 1998). This cosmic-shear–induced curl can thus be confused with that due to gravitational waves. In principle, the two can be distinguished because of their different power spectra, as shown in Fig. 2, but if the IGW amplitude is small, then the separation becomes more difficult. Lewis et al. (2002), Kesden et al. (2002), and Knox & Song (2002) showed that when the cosmic-shear confusion is taken into account, the smallest detectable inflationary energy scale is $\simeq 4 \times 10^{15}$ GeV.

The deflection angle due to cosmic shear can in principle be mapped as a function of position on the sky by studying higher-order correlations in the measured CMB temperature and polarization (Seljak & Zaldarriaga 1999; Hu 2001a; Hu 2001b; Hu & Okamoto 2002; Cooray & Kesden 2002). If this deflection angle is determined, then the polarization can be corrected and the polarization pattern at the surface of last scatter can be reconstructed. Kesden et al. (2002) and Knox & Song (2002) found that with such a reconstruction, the cosmic-shear–induced CMB curl component can be reduced by roughly a factor of ten, as indicated in Fig. 2. This then leads to a smallest inflationary energy scale that will produce a detectable IGW signal in the CMB polarization curl. The conclusion is that the CMB-polarization signature of IGWs will be undetectable, even with perfect detectors, if the energy scale of inflation is smaller than 2×10^{15} GeV.

Let us now suppose that this curl component was indeed detected. It would immediately tell us that the vacuum-energy density during inflation was $(10^{15-16}\,{\rm GeV})^4$, and thus that inflation probably had something to do with grand unification. However, there is possibly more that we can learn. Since the unifying high-energy physics responsible for inflation presumably encompasses electroweak interactions as a low-energy limit, and since the weak in-

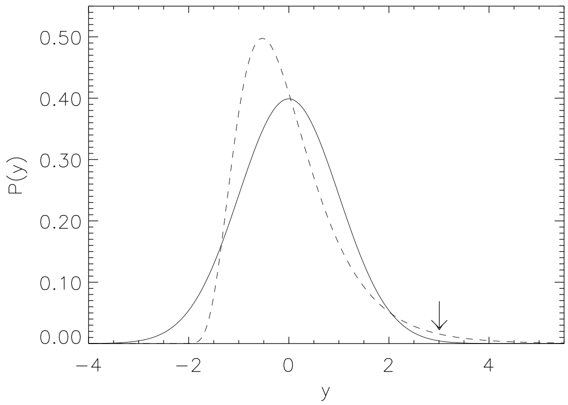

Fig. 3. The solid curve shows a Gaussian distribution $P(y)$ with unit variance, while the broken curve shows a non-Gaussian distribution with the same variance but 10 times as many peaks with $y > 3$. This illustrates (a) how the cluster abundance can be dramatically enhanced with long non-Gaussian tails (since clusters form from rare peaks); and (b) that the dispersion of y for $y > 3$ is much larger for the non-Gaussian distribution than it is for the Gaussian distribution, and this will lead to a larger scatter in the formation redshifts and sizes of clusters of a given mass. From Verde et al. (2001b).

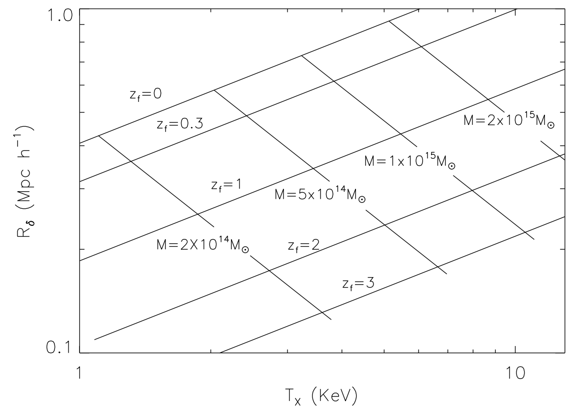

Fig. 4. Mass and formation-redshift contours in the size-temperature plane for $\Omega_0 = 0.3$ and $h = 0.65$ obtained from the spherical-top-hat model of gravitational collapse discussed in the text. It is clear from the figure that a narrow (broad) spread in the formation redshift will yield a tight (broad) size-temperature relation. For larger Ω_0, the $z_f = 0$ contour remains the same, but the spacing between equi-z_f contours increases. From Verde et al. (2001b).

teractions are parity violating, it is not unreasonable to wonder whether the physics responsible for inflation is parity violating. Lue et al. (1998) and Lepora (1998) showed how parity-violating observables could be constructed from a CMB temperature-polarization map. Moreover, examples were provided of parity-violating terms in the inflaton Lagrangian that would give rise to such signatures by, for example, producing a preponderance of right- over left-handed gravitational waves.

3. NON-GAUSSIAN INITIAL CONDITIONS

The simplest single-scalar-field inflation models predict that primordial perturbations have nearly Gaussian initial conditions. A small degree of non-Gaussianity generally arises from self-coupling of the inflaton field, but this is expected to be very tiny (Salopek et al. 1989; Salopek 1992; Falk et al. 1993; Gangui et al. 1994; Gangui 1994). More complicated models of inflation, such as two-field (Bartolo et al. 2002), warm (Gupta et al. 2002), or curvaton (Lyth et al. 2002) models may have small deviations from perfectly Gaussian initial conditions, and higher-order calculations of perturbation production suggest that non-Gaussianity may be significant even in slow-roll models (Acquaviva et al. 2002). Although it is difficult, if not impossible, to predict the exact amplitude and precise form of non-Gaussianity from inflation, it is certainly reasonable to search for it.

Perhaps the most intuitive place to look for primordial non-Gaussianity is in the CMB. Since the CMB temperature fluctuations probe directly primordial density perturbations, non-Gaussianity in the density field should lead to proportionate non-Gaussianity in the temperature maps. So, for example, if the primordial distribution of perturbations is skewed, then there should be a skewness in the temperature distribution. Alternatively, one can study the effects of primordial non-Gaussianity in the distribution of mass in the Universe today. This should have the advantage that density perturbations have undergone gravitational amplification and should thus have a larger amplitude than in the early Universe. However, we must keep in mind that the matter distribution today is expected to be non-Gaussian, even if primordial perturbations are Gaussian. This can be seen just by noting that gravitational infall can lead to regions—e.g., galaxies or clusters—with densities of order 200 times the mean density, while the smallest underdensity, a void, has a fractional underdensity of only -1. However, non-Gaussianity in the galaxy distribution from gravitational infall from Gaussian initial conditions can be calculated fairly reliably (for an excellent recent review, see, e.g., Bernardeau et al. 2002), and so the distribution today can be

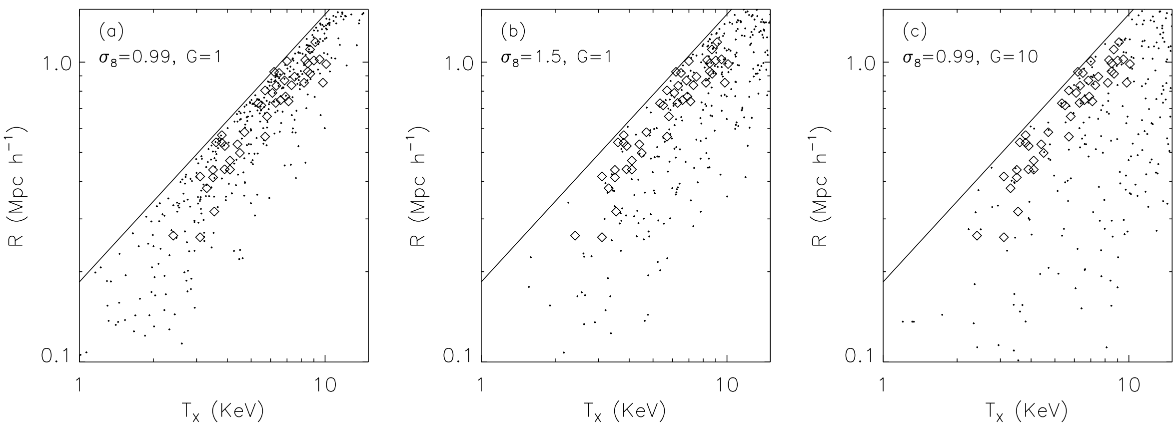

Fig. 5. (a) Size-temperature distribution for LCDM and $\sigma_8 = 0.99$ and Gaussian initial conditions. Each dot represents a simulated cluster, while the diamonds are data from M00. The line shows the size-temperature relation expected for clusters today. Panel (b) shows the same except that here we use $\sigma_8 = 1.5$. Panel (c) shows the same as in (a) but with the skew-positive distribution of Robinson et al. (2000). From Verde et al. (2001b).

checked for consistency with primordial Gaussianity. In Verde et al. (2000), we studied the relative sensitivity of galaxy surveys and CMB experiments to primordial non-Gaussianity. We considered two classes of non-Gaussianity: in the first, the gravitational potential is written $\phi(\mathbf{x},t) = g(\mathbf{x},t)+\epsilon g^2(\mathbf{x},t)$, where $g(x)$ is a Gaussian random field (so ϕ becomes Gaussian as $\epsilon \to 0$); such a form of non-Gaussianity arises in some inflation models. In the second, the fractional density perturbation is written $\delta(\mathbf{x},t) = g(\mathbf{x},t) + \epsilon g^2(\mathbf{x},t)$; this approximates the form of non-Gaussianity expected from topological defects. We then determined what the smallest detectable ϵ would be for both cases for future galaxy surveys and for CMB experiments. We found that in both cases the CMB would provide a more sensitive probe of ϵ. Conversely, if the CMB turns out to be consistent with primordial Gaussianity, then for all practical purposes, the galaxy distribution can safely be assumed to arise from Gaussian initial conditions.

Experimentally, the bispectrum from 2dF (Verde et al. 2002) and the Sloan Digital Sky Survey (Szapudi et al. 2002) have now been studied and found to be consistent with Gaussian initial conditions. A tentative claim of non-Gaussianity in the the COBE-*DMR* maps (Ferreira et al. 1998) in great excess of slow-roll-inflationary expectations (Wang & Kamionkowski 2000; Gangui & Martin 2000) was later found to be due to a very unusual and subtle systematic effect in the data (Banday et al. 2000).

The abundances of clusters provide other avenues toward detecting primordial non-Gaussianity. Galaxy clusters, the most massive gravitationally bound objects in the Universe presumably form at the highest-density peaks in the primordial density field, as indicated schematically in Fig. 3. Now suppose that instead of a Gaussian primordial distribution, we had a distribution with positive skewness, as shown in Fig. 3. In this case, we would expect there to be more high-density peaks, even for a distribution with the same variance, and thus more clusters (Robinson et al. 2000). Thus, the cluster abundance can be used to probe this type of primordial non-Gaussianity.

Just as clusters are rare objects in the Universe today, galaxies were rare at redshifts $z \gtrsim 3$. In (Verde et al. 2001a), we considered the use of abundances of high-redshift galaxies as probes of primordial non-Gaussianity. We also found an expression that relates the excess abundance of rare objects to the ϵ parameter in the models discussed above and were thus able to compare the sensitivities of cluster and high-redshift-galaxy counts and the CMB to non-Gaussianity in the models considered above. We found that although the CMB was expected to be superior in detecting non-Gaussianity in the gravitational potential, the high-redshift-galaxy abundances may do better with non-Gaussianity in the density field.

In addition to producing more clusters, such a skew-positive distribution might change the distribution of the properties of such objects. In Verde et al. (2001b), we considered the size-temperature relation. If we model the formation of a cluster as a spherical top-hat collapse, then the virial radius and the virial temperature can be determined as a function of the halo mass and the collapse redshift. We then modeled the x-ray-emitting gas to relate its size and temperature to the virial radius and temperature of the halo in which it lives in order to obtain better estimates for the x-ray isophotal radii and x-ray temperatures that are measured. Fig. 4 shows resulting contours of constant mass and constant collapse redshift in the cluster size-temperature plane. As shown there, halos that collapse earlier should lead to hotter and smaller clusters, and more massive halos should be hotter and bigger. If the primordial distribution is skew-positive, then the halos that house clusters will collapse over a wider range of redshifts, and as indicated in Fig. 5, this will lead to a broader scatter than in the size-temperature relation than is observed. In this way, primordial distributions with a large positive skewness can be constrained.

4. BROKEN SCALE INVARIANCE AND GALACTIC SUBSTRUCTURE

The final probe of inflation that we will discuss here is motivated by the galactic-substructure problem. N-body simulations of structure formation with a standard inflation-inspired scale-free spectrum of primordial perturbations predict far more substructure, in the form of dwarf galaxies, in galactic halos than is observed in the Milky Way halo, as indicated in Fig. 8 (Klypin et al. 1999; Moore et al. 1999). Although a number of possible astrophysical mechanisms for suppressing this small-scale power have been proposed (e.g., Bullock et al. 2000; Benson et al. 2002; Stoehr et al. 2002), there is still no general consensus on whether they are sufficiently effective to eliminate the problem.

Another possible explanation of the observed dearth of dwarf galaxies is a small-scale suppression of power that could occur if the inflaton potential has a sharp feature, like that shown in Fig. 7 (Kamionkowski & Liddle 2000; Yokoyama 2000). According to inflation, primordial density perturbations are produced by quantum fluctuations in the inflaton, the scalar field responsible for inflation. Moreover, the details of the power spectrum $P(k)$ of density perturbations (as shown in Fig. 6) is determined by the shape $V(\phi)$ of the inflaton potential. The amplitude of a given Fourier mode of the density field is proportional to the value of $V^{3/2}/V'$, where V' is the first derivative of the inflaton potential, at the time that the perturbation exited the horizon. In most models, the inflaton potential is smooth and

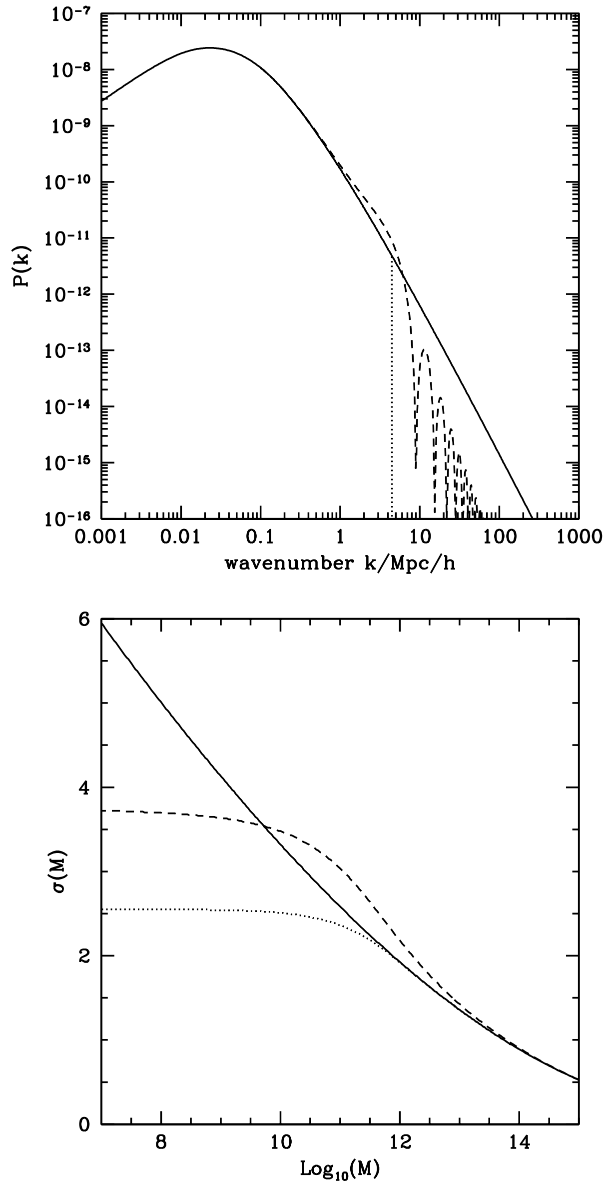

Fig. 6. The upper panel shows the power spectrum for an LCDM model (solid curve), for a model in which the power spectrum is arbitrarily cut off at $k = 4.5\,h$ Mpc^{-1} (dotted curve), and the broken-scale-invariance inflation model (dashed curve). The lower panel shows the rms mass fluctuation as a function of the enclosed mean mass M for these three models. From Kamionkowski & Liddle (2000).

this leads to a power spectrum of perturbations that is very nearly a power law—Ref. (Lidsey et al. 1997) explains very nicely how the amplitude and slope of the inflaton potential can be reconstructed in this case.

However, suppose that for some reason there is

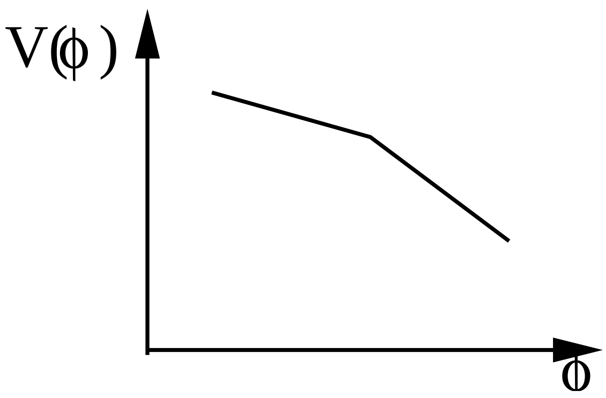

Fig. 7. An inflaton potential with a break in the first derivative.

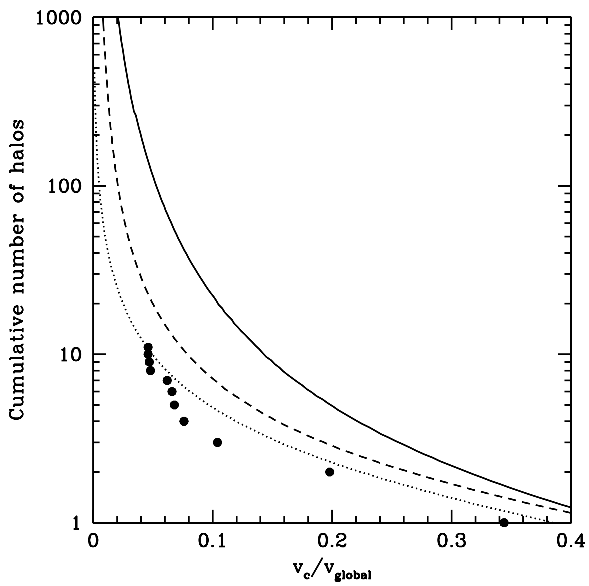

Fig. 8. The cumulative number of mini-halos for the power spectra shown in Fig. 2 as a function of the circular speed v_c of the halo divided by the circular speed $v_{\rm global}$ of the Galactic halo. The points show the Milky Way satellites. From Kamionkowski & Liddle (2000), after Moore et al. (1999).

a break in the inflaton potential, as shown in Fig. 7, and the slope increases suddenly as the inflaton roles down the potential. In this case, V' increases suddenly, and since the density-perturbation amplitude is $\propto 1/V'$, the density-perturbation amplitude on small scales (those that exit the horizon last) will be suppressed, as indicated by the dashed curve in Fig. 6. The wiggles in the dashed curve are ringing in Fourier space that results from the sharpness of the feature. If it is smoothed out, then a power spectrum more like the dotted curve in Fig. 6 becomes possible.

With the three power spectra in the upper panel of Fig. 6, the rms mass fluctuation $\sigma(M)$ on a mass scale M can be calculated, as shown in the lower panel of Fig. 6. With the scale-invariant spectrum, $\sigma(M)$ keeps rising as we go to smaller and smaller masses, leading to substructure on smaller scales. However, if power is suppressed on small scales, then $\sigma(M)$ ceases to rise (or rises only very slowly) at small M implying the absence (or suppression) of halos of these small masses.

Given $\sigma(M)$ for these three power spectra, the abundance of sub-halos in a typical galaxy-mass halo of $10^{12}\,M_\odot$ can be calculated with the extended Press-Schechter formalism. Results of this calculation are shown in Fig. 8. As a check, the approximation reproduces well the numerical-simulation results for the scale-free spectrum. For the power spectra with broken scale invariance, the abundance of low-mass substructure is reduced and brought into reasonable agreement with the observed ten or so Milky Way satellites, without violating consistency with constraints from the Lyman-alpha forest (Kamionkowski & Liddle 2000; White & Croft 2000).

Is such a break to be expected theoretically? Probably not, and there are probably simpler explanations for the shortfall that involve more conventional astrophysics. Still, these calculations show that by studying and understanding galactic substructure, we learn about the shape of the inflaton potential toward the end of inflation in a way that complements the information from earlier epochs of inflation that comes from larger scales.

5. COMMENTS

In this talk, I have briefly reviewed several avenues for probing some of the non-standard predictions of inflation. There are yet other tests—in particular, searches for a small entropy component of primordial perturbations—that I have not had time to discuss. Since our current models of inflation, as successful as they may be in terms of the flatness and primordial perturbations, are really no more than toy models, any realistic model of inflation must be, in some sense, non-standard. Although I believe that forthcoming CMB satellite experiments are likely to further confirm a flat Universe, small deviations from the toy model must sooner or later arise. Unfortunately, no single inflation model is sufficiently well motivated to predict with any certainty the existence or detectability of any of these signatures. However, as we press forward with the study of galactic structure and formation, large-scale structure, and the

CMB, we will inevitably develop the capabilities for learning more about inflation.

I thank my collaborators on the work reported here, and I acknowledge the hospitality of the Kavli Institute for Theoretical Physics. This work was supported at Caltech by NSF AST-0096023, NASA NAG5-9821, and DoE DE-FG03-92-ER40701, and at the KITP by NSF PHY99-07949.

REFERENCES

Abbott, L. F. & Wise, M. 1984, Nucl. Phys., B244, 541
Acquaviva, V., et al. 2002, astro-ph/0209156
Albrecht, A. & Steinhardt, P. J. 1982, Phys. Rev. Lett., 48, 1220
Banday, A. J., Zaroubi, S., Górski, K. M. 2000, ApJ, 533, 575
Bardeen, J. M, Steinhardt, P. J, & Turner M. S. 1983, Phys. Rev. D, 46, 645
Bartolo, N., Matarrese, S., & Riotto, A. 2002, Phys. Rev. D, 65, 103505
Benson, A. J., et al. 2002, MNRAS, 333, 177
Bernardeau, F., et al. 2002, Phys. Rep., 367, 1
de Bernardis, P., et al. 2002, Nature, 404, 955
Bullock, J. S., Kravtsov, A. V., & Weinberg, D. H. 2000, ApJ, 539, 517
Cooray, A. & Kesden, M., 2002, astro-ph/0204068
Falk, T., Rangarajan, R., & Srednicki, M. 1993, ApJ, 403, L1
Ferreira, P. G., Magueijo, J., & Górski, K. M. 1998, ApJ, 503, L1
Gangui, A., et al. 1994, ApJ, 430, 447
Gangui, A. 1994, Phys. Rev. D, 50, 3684
Gangui, A. & Martin, J. 2000, MNRAS, 313, 323
Gupta, S., et al. 2002, Phys. Rev. D, 66, 043510
Guth, A. H. 1981, Phys. Rev. D, 28, 347
Guth, A. H & Pi, S.-Y. 1982, Phys. Rev. Lett., 49, 1110
Halverson, N. W., et al. 2002, ApJ, 568, 38
Hanany, S., et al. 2000, ApJ, 545, L5
Hawking, S. W. 1982, Phys. Lett., B115, 29
Hu, W. 2001a, Phys. Rev. D, 64, 083005
Hu, W. 2001b, ApJ, 557, L79
Hu, W. & Okamoto, T. 2002, ApJ, 574, 566
Jaffe, A. H., Kamionkowski, M., & Wang, L. 2000, Phys. Rev. D, 61, 083501
Kamionkowski, M., Kosowsky, A., & Stebbins, A. 1997a, Phys. Rev. Lett., 78, 2058.
Kamionkowski, M., Kosowsky, A., & Stebbins, A. 1997b, Phys. Rev. D, 55, 7368
Kamionkowski, M. & Kosowsky, A. 1998, Phys. Rev. D, 67, 685
Kamionkowski, M. & Kosowsky, A. 1999, Ann. Rev. Nucl. Part. Sci., 49, 77
Kamionkowski, M. & Liddle, A. R., 2000, Phys. Rev. Lett., 84, 4525
Kesden, M., Cooray, A., & Kamionkowski, M. 2002, Phys. Rev. Lett., 89, 011304
Klypin, A. A., Kravtsov, A. V., & Valenzuela, O. 1999, ApJ, 522, 82
Knox, L. & Song, Y.-S. 2002, Phys. Rev. Lett., 89, 011303
Lepora, N., qr-qc/9812077
Lewis, A., Challinor, A., & Turok, N. 2002, Phys. Rev. D, 65, 023505
Linde, A. D. 1982a, Phys. Lett., B108 389
Linde, A. D. 1982b, Phys. Lett., B116, 335
Lidsey, J. E., et al. 1997, Rev. Mod. Phys., 69, 373
Lue, A., Wang, L., & Kamionkowski, M. 1998, Phys. Rev. Lett., 83, 1503
Lyth, D., Ungarelli, C., & Wands, D. 2002, astro-ph/0208055
Mason, B. S., et al., astro-ph/0205384
Miller, A. D., et al. 1999, ApJ, 524, L1
Moore, B., et al. 1999, ApJ, 524, L19
Robinson, J., Gawiser, E., & Silk, J. 2002, ApJ, 2000, 532, 1
Salopek, D. S., Bond, J. R., & Bardeen, J. M. 1989, Phys. Rev. D, 40, 1753
Salopek, D. S. 1992, Phys. Rev. D, 45, 1139
Seljak, U. & Zaldarriaga, M. 1997, Phys. Rev. Lett., 78, 2054
Seljak, U. & Zaldarriaga, M. 1999, Phys. Rev. Lett., 82, 2636
Starobinsky, A. A. 1982, Phys. Lett., B117, 175
Stoehr, F., et al. 2002, astro-ph/0203342.
Szapudi, I., et al. 2002, ApJ, 570, 75
Verde, L., et al. 2000, MNRAS, 313, L141
Verde, L., et al. 2001, MNRAS, 325, 412
Verde, L., et al. 2001, MNRAS, 321, L7
Verde, L., et al. 2002, MNRAS, 335, 432
Wang, L. & Kamionkowski, M. 2000, Phys. Rev. D, 61, 063504
White, M. & Croft, R. A. C. 2000, ApJ, 539, 497
Yokoyama, J. 2000, Phys. Rev. D, 62, 123509
Zaldarriaga, M. & Seljak, U. 1997, Phys. Rev. D, 55, 1830
Zaldarriaga, M. & Seljak, U. 1998, Phys. Rev. D, 58, 023003

California Institute of Technology, Mail Code 130-33, Pasadena, CA 91125, USA (kamion@tapir.caltech.edu).